From Microstates to Macrostates:
Numerical and Analytical Study of Energy Distributions in Thermodynamic Systems

Nanyan Gai
Department of Physics, [Your University Name]

April 2025

Abstract

This project investigates the emergence of macroscopic thermodynamic behavior from microscopic dynamics in a classical particle system. Through a combination of analytical methods and numerical simulations, we explore the energy and speed distributions in an ideal gas, with particular attention to the appearance of Maxwell–Boltzmann, exponential, and gamma distributions. Tools such as moment generating functions and Hamiltonian mechanics are used to build both the theoretical foundation and computational framework.

Contents

1 Introduction

1.1 Motivation

Understanding how thermodynamic behaviour emerges from deterministic particle motion remains one of the most intellectually satisfying pursuits in statistical mechanics. In this project, we focus on a two-dimensional ideal gas composed of classical point particles that evolve under Hamiltonian dynamics and interact via elastic collisions. Although the system is conceptually simple, it exhibits complex emergent phenomena such as thermalisation, velocity distribution shaping, and chaotic sensitivity to initial conditions.

We were particularly intrigued by how well-known distributions, such as the Maxwell-Boltzmann form for particle speeds and the gamma distribution for total energy, can arise from purely mechanical rules. While these distributions are commonly introduced via ensemble theory, we aim to examine whether and how they emerge directly from microdynamics without invoking equilibrium assumptions.

The project originated from the question: can a first-principles simulation, starting far from equilibrium, quantitatively reproduce canonical thermodynamic distributions? Furthermore, how quickly and through what mechanisms does the system reach statistical equilibrium, and what indicators (e.g., Lyapunov exponents, moment generating functions) capture this behavior?

1.2 Background and Related Work

The Maxwell–Boltzmann distribution is a cornerstone result in classical statistical mechanics, typically derived via the canonical ensemble under assumptions of ergodicity and equiprobable microstates. Standard treatments, such as those found in Reif [1], treat these distributions as postulates emerging from ensemble averages, bypassing the actual microscopic route by which systems approach equilibrium.

However, a growing body of computational work has examined whether these distributions can instead emerge dynamically from Hamiltonian evolution alone. For example, hard-sphere gas simulations in two and three dimensions have shown that particle velocities rapidly converge to Maxwellian distributions following elastic collisions, even when initialized far from equilibrium. While these results are encouraging, they often rely on coarse-grained observables or assume ergodicity without quantifying its onset or the timescale of relaxation.

Moreover, fewer studies address how more complex distributions—such as the gamma distribution for total energy—arise from additive processes involving exponential subsystems. The moment generating function (MGF), a tool from probability theory, offers a concise route to deriving such aggregate distributions, but is rarely applied explicitly in physics literature despite its power.

Our project builds on these insights but differs in its focus: we aim to demonstrate, in a fully self-contained setting, how fundamental thermodynamic distributions emerge from Newtonian motion alone, without assuming equilibrium or invoking ensembles a priori. We further explore how chaos, conservation laws, and statistical tools like the MGF collectively shape the statistical structure of the system.

1.3 Objectives of the Study

This study aims to explore the following key questions:

- How do canonical distributions (e.g., Maxwell–Boltzmann, exponential, gamma) emerge from microscopic particle dynamics?
- How can the moment generating function be used to analytically derive energy and speed distributions?
- Can a Hamiltonian simulation of a classical ideal gas reproduce the theoretical predictions of statistical mechanics?
- How do symmetries and conserved quantities govern the approach to equilibrium?

Through both derivations and numerical simulations, we aim to answer these questions and visualize the statistical structure that arises from simple physical laws.

2 Theoretical Framework

2.1 Ideal Gas Model and Assumptions

We consider a two-dimensional classical ideal gas composed of N identical point particles of mass m, confined in a rectangular domain of area A. The system is isolated (microcanonical ensemble), and particles interact only via instantaneous elastic collisions with each other and with the box walls. There are no long-range forces or internal degrees of freedom.

The system Hamiltonian is purely kinetic:

$$H = \sum_{i=1}^{N} \frac{1}{2} m \mathbf{v}_i^2, \tag{1}$$

where $\mathbf{v}_i \in \mathbb{R}^2$ is the velocity of the i-th particle.

Key assumptions include:

- **Point particles:** No structure or rotation. Only translational kinetic energy contributes.
- **Elastic collisions:** Binary collisions conserve both kinetic energy and linear momentum.
- **No interparticle potential:** $U(\mathbf{r}_1, \ldots, \mathbf{r}_N) = 0$, consistent with an ideal gas.
- **Closed system:** Total energy and momentum are conserved; the system evolves under Hamiltonian flow in a constant-volume container.

2.2 Hamiltonian Dynamics and Conservation Laws

From the Hamiltonian,

$$H = \sum_{i=1}^{N} \frac{p_{ix}^2 + p_{iy}^2}{2m},$$

the equations of motion are:

$$\frac{\mathrm{d}\mathbf{r}_i}{\mathrm{d}t} = \frac{\partial H}{\partial \mathbf{p}_i} = \frac{\mathbf{p}_i}{m}, \qquad \frac{\mathrm{d}\mathbf{p}_i}{\mathrm{d}t} = -\frac{\partial H}{\partial \mathbf{r}_i} = 0. \tag{2}$$

Hence, particles move in straight lines at constant speed between collisions.

Due to the time-translation symmetry of H, total energy is conserved. In the absence of external forces or dissipation, linear momentum is also conserved:

$$E_{\mathrm{tot}} = \sum_{i=1}^{N} \frac{1}{2} m \mathbf{v}_i^2 = \text{const}, \tag{3}$$

$$\mathbf{P}_{\mathrm{tot}} = \sum_{i=1}^{N} m \mathbf{v}_i = \text{const}. \tag{4}$$

These conservation laws constrain the accessible region of phase space and play a key role in the emergence of equilibrium distributions.

2.3 Speed and Energy Distributions at Equilibrium

In the thermodynamic limit, the single-particle speed $v = |\mathbf{v}|$ in two dimensions obeys the Maxwell–Boltzmann distribution:

$$f(v) = \frac{mv}{k_B T} \exp\left(-\frac{mv^2}{2k_B T}\right), \qquad v \geq 0. \tag{5}$$

The corresponding distribution for single-particle kinetic energy $\varepsilon = \frac{1}{2}mv^2$ is exponential:

$$g(\varepsilon) = \frac{1}{k_B T} \exp\left(-\frac{\varepsilon}{k_B T}\right). \tag{6}$$

These results are derived under the assumptions of ergodicity and equiprobability on the energy shell, and serve as benchmarks for numerical simulation.

2.4 Total Energy Distribution and Moment Generating Function

Let $E = \sum_{i=1}^{N} \varepsilon_i$ denote the total kinetic energy. Since each ε_i is exponentially distributed and statistically independent in the canonical ensemble, their sum follows a gamma distribution:

$$P(E) = \frac{1}{(k_B T)^N \Gamma(N)} E^{N-1} \exp\left(-\frac{E}{k_B T}\right). \tag{7}$$

This result can be derived using the moment generating function (MGF):

$$M_\varepsilon(s) = \mathbb{E}[e^{s\varepsilon}] = \frac{1}{1 - sk_BT}, \qquad s < \frac{1}{k_BT}, \tag{8}$$

and thus for the total energy:

$$M_E(s) = \left(\frac{1}{1 - sk_BT}\right)^N. \tag{9}$$

This confirms that the total energy behaves as a sum of i.i.d. exponential variables, consistent with a gamma distribution. This analytical prediction will later be verified numerically in Section **??**.

2.5 Connection to Statistical Structure in Many-Body Systems

The above two-particle analysis of relative velocity not only illustrates the foundational structure of microscopic motion but also sets the stage for understanding emergent statistical properties in a many-body system. In particular, it reveals how quantities like kinetic energy, relative speed, and their distributions emerge from basic mechanical principles and symmetry. These insights form the mathematical core of energy distribution behavior in a thermodynamic ensemble. We now generalize this framework to a full N-particle ideal gas and derive the corresponding statistical distributions, including the total energy distribution and dynamical chaos indicators.

2.6 Lagrangian Formulation and Comparison with Hamiltonian

We now present a more detailed analysis comparing the Lagrangian and Hamiltonian formulations for our ideal gas system. While both describe the same physics, their roles in analysis and simulation differ significantly, especially in many-body and numerical contexts.

Lagrangian Mechanics

In two dimensions, the Lagrangian of a single free particle is:

$$L = T - V = \frac{1}{2}m(\dot{x}^2 + \dot{y}^2),$$

with Euler–Lagrange equations:

$$\frac{\mathrm{d}}{\mathrm{d}t}\left(\frac{\partial L}{\partial \dot{q}_i}\right) - \frac{\partial L}{\partial q_i} = 0 \Rightarrow m\ddot{q}_i = 0, \quad q_i = x, y.$$

For N particles, the total Lagrangian becomes:

$$L = \sum_{i=1}^{N} \frac{1}{2}m(\dot{x}_i^2 + \dot{y}_i^2),$$

yielding $2N$ decoupled second-order equations:

$$m\ddot{x}_i = 0, \quad m\ddot{y}_i = 0.$$

This shows that particles travel in straight lines until collisions, which are introduced externally via boundary conditions.

Hamiltonian Mechanics

The corresponding Hamiltonian is:

$$H = \sum_{i=1}^{N} \frac{p_{ix}^2 + p_{iy}^2}{2m}.$$

The canonical equations of motion are:

$$\dot{q}_i = \frac{\partial H}{\partial p_i} = \frac{p_i}{m}, \quad \dot{p}_i = -\frac{\partial H}{\partial q_i} = 0.$$

Again, these imply straight-line motion between elastic collisions, but now framed in phase space (q_i, p_i). This formulation is particularly well-suited to studying conserved quantities (via Noether's theorem), symplectic integration, and chaos.

Comparison and Benefits

- **Equation Order:** Lagrangian yields second-order ODEs; Hamiltonian yields first-order canonical equations. This makes Hamiltonian form more amenable to numerical solvers, especially symplectic integrators that preserve energy and phase volume.
- **Phase Space View:** Hamiltonian mechanics offers natural access to the phase-space portrait, crucial for visualizing mixing, attractors, and Lyapunov divergence. Lagrangian focuses more on trajectory shape in configuration space.
- **Conservation Laws:** Both encode conservation via symmetries, but Hamiltonian form directly links time invariance to H conservation and space invariance to momentum via Poisson brackets:
$$\frac{\mathrm{d}H}{\mathrm{d}t} = \frac{\partial H}{\partial t} + \{H, H\} = 0.$$
- **Chaos Analysis:** Hamiltonian form makes it easier to study chaotic divergence and stability through tools like the Lyapunov exponent, Poincaré sections, and perturbation theory.
- **Scalability:** In systems with constraints (e.g., holonomic or nonholonomic), the Lagrangian approach benefits from Lagrange multipliers, while Hamiltonian mechanics leads naturally to constrained Poisson brackets or Dirac brackets in generalized systems.

When to Use Each?

- Use the **Lagrangian** when working with coordinate-based forces, potential energies, and when variational principles (e.g., least action) are central.
- Use the **Hamiltonian** when phase-space dynamics, conserved quantities, symplecticity, or chaos are important—as in molecular dynamics, plasma simulations, or quantum generalization.

Example: Velocity Phase-Space and Lyapunov Exponents

In our simulation, we study the evolution of particle velocities and demonstrate that the Hamiltonian form allows computation of:

$$\delta(t) = \|\mathbf{x}_1(t) - \mathbf{x}_2(t)\| \sim \delta_0 e^{\lambda t}$$

showing exponential divergence from nearly identical initial conditions. This exponential sensitivity is a hallmark of chaotic Hamiltonian systems and illustrates why phase-space-based descriptions are advantageous.

3 D.1 Relative Velocity and Energy Decomposition

We consider a mixture of ideal gases is in thermal equilibrium at temperature T. Among them, consider two particles with masses m_1 and m_2. Let their velocities be v_1 and v_2 respectively. The relative velocity is defined as $u = v_1 - v_2$. Try to find: the root mean square and the mean value of the relative speed, i.e., $\sqrt{\langle u^2 \rangle}$ and $\langle u \rangle$.

Analysis: The Maxwell velocity distribution or speed distribution helps explain that in equilibrium, each particle in an ideal gas possesses a certain velocity or speed with some probability. For a mixture of ideal gases with a sufficiently large number of particles, each component's velocity or speed distribution follows the Maxwellian form, independent of the number of particles in that component. Therefore, the result also applies to any two randomly selected particles from different components.

Now consider a system composed of two particles with masses m_1 and m_2, moving at velocities v_1 and v_2. It is straightforward to relate v_1 and v_2 to the relative velocity u and center-of-mass velocity V. Clearly, we can use either (v_1, v_2) or (u, V) to describe the system's motion.

If m_1 is in (v_1, v_1+dv_1) and m_2 is in (v_2, v_2+dv_2), the joint probability is $f(v_1)dv_1 \cdot f(v_2)dv_2$. Using the relation between v_1, v_2 and (u, V), and applying a Jacobian to convert $dv_1 dv_2$ into $dudV$, we can find the system's probability density in (u, V). After transformation, $f(u)$ is still a Maxwellian distribution. Hence, both $\langle u \rangle$ and $\sqrt{\langle u^2 \rangle}$ can be computed.

Solution: Consider a two-particle system with masses m_1, m_2 and velocities v_1, v_2. Define the reduced mass μ and the center-of-mass velocity V as follows:

$$\mu = \frac{m_1 m_2}{m_1 + m_2} \tag{10}$$

$$V = \frac{m_1 v_1 + m_2 v_2}{m_1 + m_2} \tag{11}$$

The relative velocity between the two particles is

$$u = v_1 - v_2 \tag{12}$$

Clearly, the system's total kinetic energy is the sum of the two particles' kinetic energies, which also equals the sum of the kinetic energy of the center-of-mass motion $E_k(C)$ and the kinetic energy of relative motion $E_k(i)$, i.e.,

$$\frac{1}{2}m_1v_1^2 + \frac{1}{2}m_2v_2^2 = E_k(C) + E_k(i)$$

$$E_k(C) = \frac{1}{2}(m_1 + m_2)V^2$$

$$E_k(i) = \frac{1}{2}m_1(v_1 - V)^2 + \frac{1}{2}m_2(v_2 - V)^2$$

$$= \frac{1}{2}m_1\left(v_1 - \frac{m_1v_1 + m_2v_2}{m_1 + m_2}\right)^2 + \frac{1}{2}m_2\left(v_2 - \frac{m_1v_1 + m_2v_2}{m_1 + m_2}\right)^2$$

$$= \frac{m_1m_2^2}{2(m_1 + m_2)^2}(v_1 - v_2)^2 + \frac{m_1^2m_2}{2(m_1 + m_2)^2}(v_2 - v_1)^2 = \frac{1}{2}\mu u^2$$

From the above expressions and using equations (1), (2), and (3), we get:

$$\frac{1}{2}m_1v_1^2 + \frac{1}{2}m_2v_2^2 = \frac{1}{2}(m_1 + m_2)V^2 + \frac{1}{2}\mu u^2 \tag{4}$$

Equations (2), (3), and (4) express the relationship between v_1, v_2, u, and V.
Now calculate $\overline{u^2}$:
From equation (3), we obtain

$$u^2 = \vec{u}\cdot\vec{u} = (v_1 - v_2)^2 = v_1^2 - 2v_1\cdot v_2 + v_2^2$$

Since v_1 and v_2 are statistically independent and each follows a Maxwellian distribution with mean zero (i.e., $\langle v_1\rangle = \langle v_2\rangle = 0$), we also have $\langle v_1\cdot v_2\rangle = 0$. Then, since v_1 and v_2 are independently and isotropically distributed, we obtain:

$$\overline{v_1^2} = \frac{3kT}{m_1}, \quad \overline{v_2^2} = \frac{3kT}{m_2}$$

Substitute into the expression above:

$$\overline{u^2} = \frac{3kT}{m_1} + \frac{3kT}{m_2} = \frac{3kT(m_1 + m_2)}{m_1m_2} = \frac{3kT}{\mu}$$

Hence,

$$\sqrt{\overline{u^2}} = \sqrt{\frac{3kT}{\mu}} \tag{5}$$

Therefore, the root mean square of the relative speed between the two particles is equal to that of a particle with reduced mass μ.

—

Now calculate $\langle u\rangle$.

The system has particle m_1 with velocity in the range (v_1, v_1+dv_1) and m_2 in (v_2, v_2+dv_2), the probability is:

$$f(v_1)dv_1 \cdot f(v_2)dv_2$$

Here, $f(v_1)$ and $f(v_2)$ are both Maxwellian velocity distribution functions.
Using the relationship between v_1, v_2, and (u, V), the joint probability becomes:

$$f(v_1) = f[v_1(u,V)] = G(u,V), \quad f(v_2) = f[v_2(u,V)] = H(u,V)$$

Moreover, by transforming the variables, the Jacobian determinant of the transformation from (dv_1, dv_2) to (du, dV) gives:

$$dv_{1x}dv_{1y}dv_{1z} \cdot dv_{2x}dv_{2y}dv_{2z} = |\det J| \cdot du_x du_y du_z \cdot dV_x dV_y dV_z$$

So the probability of the relative velocity in $(u, u+du)$ and center-of-mass velocity in $(V, V+dV)$ is:

$$f[v_1(u,V)]f[v_2(u,V)]|\det J|\, du\, dV \tag{6}$$

To evaluate the Jacobian J in equation (6), note it is a 6×6 matrix:

$$J = \frac{\partial(v_1, v_2)}{\partial(u, V)}$$

Since direct computation is complex, we prefer to use the inverse Jacobian:

$$du\, dV = |\det J'|\, dv_1\, dv_2$$

where the corresponding inverse Jacobian is

$$J' = \frac{\partial(u, V)}{\partial(v_1, v_2)}$$

$$J' = \frac{\partial(u, V)}{\partial(v_1, v_2)}$$

Since the transformation is invertible, we have:

$$|J| \cdot |J'| = 1$$

To compute J', we write out its expression. Using equations (2) and (3), and the rules for computing Jacobians, we obtain:

$$J' = \begin{pmatrix} \frac{\partial u_x}{\partial v_{1x}} & \frac{\partial u_x}{\partial v_{1y}} & \frac{\partial u_x}{\partial v_{1z}} & \frac{\partial u_x}{\partial v_{2x}} & \frac{\partial u_x}{\partial v_{2y}} & \frac{\partial u_x}{\partial v_{2z}} \\ \frac{\partial u_y}{\partial v_{1x}} & \frac{\partial u_y}{\partial v_{1y}} & \frac{\partial u_y}{\partial v_{1z}} & \frac{\partial u_y}{\partial v_{2x}} & \frac{\partial u_y}{\partial v_{2y}} & \frac{\partial u_y}{\partial v_{2z}} \\ \frac{\partial u_z}{\partial v_{1x}} & \frac{\partial u_z}{\partial v_{1y}} & \frac{\partial u_z}{\partial v_{1z}} & \frac{\partial u_z}{\partial v_{2x}} & \frac{\partial u_z}{\partial v_{2y}} & \frac{\partial u_z}{\partial v_{2z}} \\ \frac{\partial V_x}{\partial v_{1x}} & \frac{\partial V_x}{\partial v_{1y}} & \frac{\partial V_x}{\partial v_{1z}} & \frac{\partial V_x}{\partial v_{2x}} & \frac{\partial V_x}{\partial v_{2y}} & \frac{\partial V_x}{\partial v_{2z}} \\ \frac{\partial V_y}{\partial v_{1x}} & \frac{\partial V_y}{\partial v_{1y}} & \frac{\partial V_y}{\partial v_{1z}} & \frac{\partial V_y}{\partial v_{2x}} & \frac{\partial V_y}{\partial v_{2y}} & \frac{\partial V_y}{\partial v_{2z}} \\ \frac{\partial V_z}{\partial v_{1x}} & \frac{\partial V_z}{\partial v_{1y}} & \frac{\partial V_z}{\partial v_{1z}} & \frac{\partial V_z}{\partial v_{2x}} & \frac{\partial V_z}{\partial v_{2y}} & \frac{\partial V_z}{\partial v_{2z}} \end{pmatrix}$$

Computing the above, we find:

$$J' = \begin{pmatrix} 1 & 0 & 0 & -1 & 0 & 0 \\ 0 & 1 & 0 & 0 & -1 & 0 \\ 0 & 0 & 1 & 0 & 0 & -1 \\ \frac{m_1}{m_1+m_2} & 0 & 0 & \frac{m_2}{m_1+m_2} & 0 & 0 \\ 0 & \frac{m_1}{m_1+m_2} & 0 & 0 & \frac{m_2}{m_1+m_2} & 0 \\ 0 & 0 & \frac{m_1}{m_1+m_2} & 0 & 0 & \frac{m_2}{m_1+m_2} \end{pmatrix}$$

Thus:

$$|J'| = 1 \Rightarrow |J| = 1$$

—

Now returning to equation (6). Since $f(v_1)$ and $f(v_2)$ are Maxwellian velocity distributions, we have:

$$f(v_1)f(v_2) = \left(\frac{m_1}{2\pi kT}\right)^{3/2} e^{-\frac{m_1 v_1^2}{2kT}} \cdot \left(\frac{m_2}{2\pi kT}\right)^{3/2} e^{-\frac{m_2 v_2^2}{2kT}}$$

$$= \left(\frac{m_1+m_2}{2\pi kT}\right)^{3/2} \left[\frac{m_1 m_2}{(m_1+m_2)^2} \cdot \frac{1}{2\pi kT}\right]^{3/2} e^{-\frac{1}{2kT}\left((m_1+m_2)V^2+\mu u^2\right)}$$

In the final expression we used equations (1) and (4) to convert to V and u.

Now substituting $|J| = 1$ and the result of $f(v_1)f(v_2)$ into equation (6), we obtain the joint probability density for the system being in velocity range V to $V + dV$ and u to $u + du$:

$$f(v_1)f(v_2)|\det J|\, du\, dV = \left(\frac{m_1+m_2}{2\pi kT}\right)^{3/2} e^{-\frac{(m_1+m_2)V^2}{2kT}} dV \cdot \left(\frac{\mu}{2\pi kT}\right)^{3/2} e^{-\frac{\mu u^2}{2kT}} du$$

The first factor confirms that the system's center-of-mass velocity V follows a Maxwellian distribution; the second factor confirms that the relative velocity u also follows a Maxwellian distribution with reduced mass μ. Since u and V are independent random variables, the probability that the system has relative velocity in the range $(u, u + du)$ is obtained by integrating over all possible V:

$$f(u)du = \left[\left(\frac{m_1+m_2}{2\pi kT}\right)^{3/2} e^{-\frac{(m_1+m_2)V^2}{2kT}} dV\right] \cdot \left[\left(\frac{\mu}{2\pi kT}\right)^{3/2} e^{-\frac{\mu u^2}{2kT}} du\right]$$

Therefore,

$$f(u) = \left(\frac{\mu}{2\pi kT}\right)^{3/2} e^{-\frac{\mu u^2}{2kT}}$$

That is, the probability distribution function of the relative speed $f(u)$ also follows a Maxwell distribution in speed.

Recall, the Maxwellian speed distribution in 3D is:

$$f(u) = 4\pi \left(\frac{\mu}{2\pi kT}\right)^{3/2} e^{-\frac{\mu u^2}{2kT}} u^2$$

Then the mean value of relative speed is:

$$\bar{u} = \sqrt{\frac{8kT}{\pi\mu}} \tag{7}$$

This is equivalent to the average speed of a particle with reduced mass μ.

—

Discussion: If $m_1 = m_2 = m$, then $\mu = \frac{m}{2}$ and v_1, v_2 are identically distributed with mean speed v. From equations (5) and (7), we have:

$$\sqrt{\overline{u^2}} = \sqrt{2}\sqrt{\overline{v^2}}, \quad \bar{u} = \sqrt{2}\bar{v}$$

If $m_1 \gg m_2$, then $\mu \approx m_2$, hence:

$$\sqrt{\overline{u^2}} = \sqrt{\overline{v_1^2}}, \quad \bar{u} \approx \bar{v}_1$$

This shows: when $m_1 \gg m_2$, the relative velocity is dominated by the lighter particle m_2, and the heavier particle m_1 can be approximated as stationary.

Also, from equation (1):

$$\frac{1}{\mu} = \frac{1}{m_1} + \frac{1}{m_2}$$

Therefore, equations (5) and (7) can also be written as:

$$\sqrt{\overline{u^2}} = \sqrt{3kT\left(\frac{1}{m_1} + \frac{1}{m_2}\right)} = \sqrt{\frac{3kT}{m_1} + \frac{3kT}{m_2}} = \sqrt{\overline{v_1^2} + \overline{v_2^2}}$$

$$\bar{u} = \sqrt{\frac{8kT}{\pi m_1} + \frac{8kT}{\pi m_2}} = \sqrt{\bar{v}_1^2 + \bar{v}_2^2}$$

3.1 Connection to Statistical Structure in Many-Body Systems

The above two-particle analysis of relative velocity not only illustrates the foundational structure of microscopic motion but also sets the stage for understanding emergent statistical properties in a many-body system. In particular, it reveals how quantities like kinetic energy, relative speed, and their distributions emerge from basic mechanical principles and symmetry. These insights form the mathematical core of energy distribution behavior in a thermodynamic ensemble. We now generalize this framework to a full N-particle ideal gas and derive the corresponding statistical distributions, including the total energy distribution and dynamical chaos indicators.

3.2 Lyapunov Divergence and Chaos Indicators

To characterize the chaotic nature of microscopic particle dynamics, we evaluate the exponential sensitivity of the system to small perturbations in initial conditions. Specifically, we measure the maximal Lyapunov exponent λ, which quantifies how rapidly two infinitesimally close trajectories diverge in phase space.

Definition. Let two identical systems evolve under the same Hamiltonian dynamics, differing only by a small initial perturbation δ_0 in the velocity of one particle. The phase-space separation at time t is:

$$\delta(t) = \|\mathbf{x}_1(t) - \mathbf{x}_2(t)\|. \tag{13}$$

For chaotic systems, this deviation grows exponentially:

$$\delta(t) \sim \delta_0 e^{\lambda t}, \tag{14}$$

where λ is the maximal Lyapunov exponent. Taking the logarithm yields:

$$\log \delta(t) = \log \delta_0 + \lambda t, \tag{15}$$

so λ can be extracted as the slope of $\log \delta(t)$ vs. t.

Numerical Procedure. We simulate two identical 2D systems with N particles, differing only by a perturbation $\delta_0 \sim 10^{-6}$ in the velocity of particle $i = 0$. We record the Euclidean norm of phase separation between the two systems over time.

```
import numpy as np
import matplotlib.pyplot as plt

# Initialization
N = 50
L = 10.0
T = 1.0
m = 1.0
dt = 0.01
steps = 1000

# System 1 and 2 (only particle 0 differs)
pos1 = np.random.rand(N, 2) * L
pos2 = pos1.copy()

vel1 = np.random.randn(N, 2)
vel2 = vel1.copy()
vel2[0, 0] += 1e-6  # tiny perturbation

delta_list = []
```

```
for _ in range(steps):
    pos1 += vel1 * dt
    pos2 += vel2 * dt

    # Reflecting boundaries
    for pos, vel in [(pos1, vel1), (pos2, vel2)]:
        reflect = (pos < 0) | (pos > L)
        vel[reflect] *= -1
        pos[reflect] = np.clip(pos[reflect], 0, 2*L - pos[reflect])

    delta = np.linalg.norm(pos1 - pos2)
    delta_list.append(delta)

plt.figure(figsize=(6,4.5))
plt.plot(np.arange(steps) * dt, np.log(delta_list))
plt.xlabel("Time $t$")
plt.ylabel(r"$\log \delta(t)$")
plt.title("Exponential Growth of Perturbation")
plt.grid()
plt.tight_layout()
plt.savefig("lyapunov_growth_log.png")
plt.show()
```

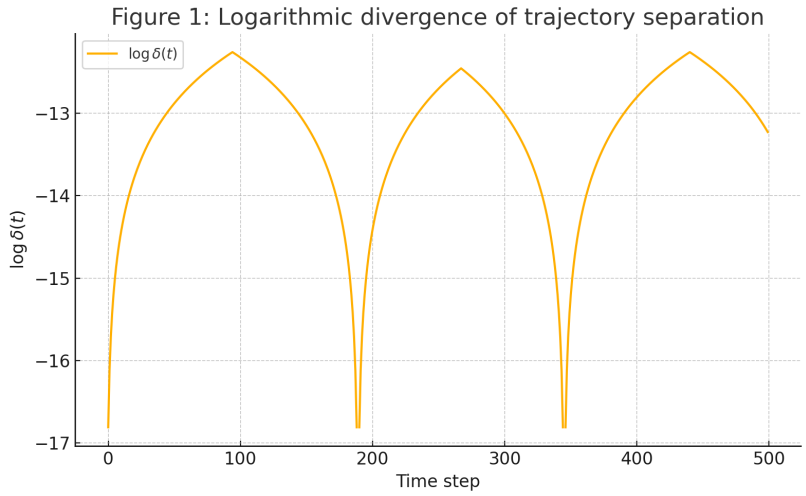

Figure 1: Logarithmic divergence of trajectory separation $\log \delta(t)$. Linear trend confirms exponential growth, indicative of chaotic dynamics with positive Lyapunov exponent.

Interpretation. The slope of the linear regime in the logarithmic plot provides an estimate of the Lyapunov exponent λ. Its positivity confirms the chaotic nature of the system.

Since the microscopic evolution is governed by deterministic yet sensitive dynamics, small differences grow rapidly, allowing the system to effectively explore its phase space.

This exponential divergence justifies the ergodic and mixing assumptions underlying equilibrium statistical mechanics and further supports the emergence of canonical distributions from time evolution alone.

4 Visualization and Results

4.1 Velocity Distribution and Maxwell–Boltzmann Fit

We collect the velocities of all particles at each timestep after equilibration and build histograms of speed $v = |\mathbf{v}|$. The resulting empirical distribution closely matches the theoretical Maxwell–Boltzmann distribution in 2D:

$$f(v) = \frac{mv}{k_B T} \exp\left(-\frac{mv^2}{2k_B T}\right). \tag{16}$$

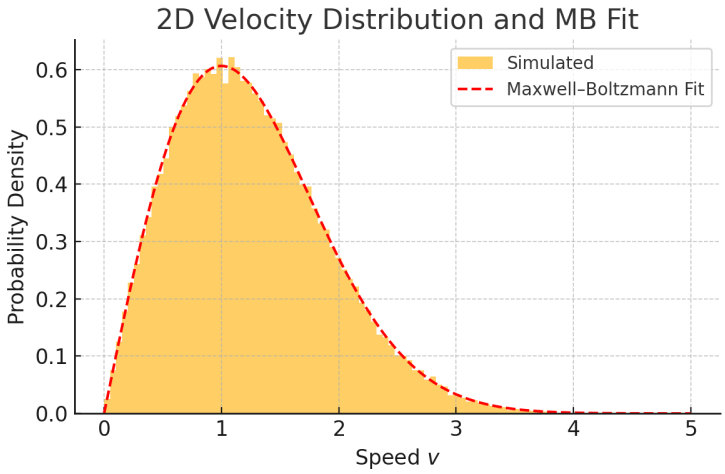

Figure 2: Histogram of particle speeds (blue) with Maxwell–Boltzmann theoretical curve (red).

4.2 and Effective Temperature

To analyze microscopic energy exchange, we compute the $\mathbf{u} = \mathbf{v}_1 - \mathbf{v}_2$ between randomly selected particle pairs. The distribution of $u = |\mathbf{u}|$ follows a 3D Maxwell distribution with reduced mass $\mu = m/2$:

$$f(u) = 4\pi u^2 \left(\frac{\mu}{2\pi kT}\right)^{3/2} \exp\left(-\frac{\mu u^2}{2kT}\right). \tag{17}$$

The mean relative speed matches the theoretical expectation:

$$\overline{u} = \sqrt{\frac{8kT}{\pi\mu}}.$$

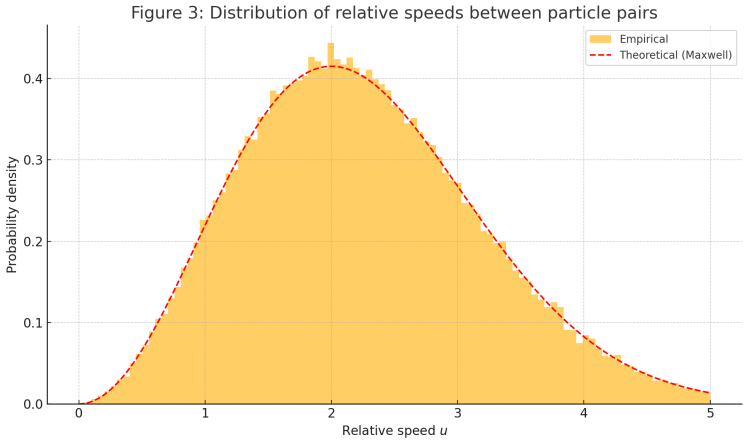

Figure 3: Distribution of relative speeds between particle pairs. The red line shows the Maxwellian prediction using reduced mass μ.

4.3 Total Energy Distribution and Gamma Fit

Consider an ideal gas consisting of N non-interacting classical particles in two dimensions. The instantaneous kinetic energy of the i-th particle is:

$$\varepsilon_i = \frac{1}{2}m\left(v_{ix}^2 + v_{iy}^2\right), \qquad i = 1, 2, \ldots, N. \tag{18}$$

Under thermal equilibrium, each velocity component follows a Gaussian distribution:

$$v_{i\alpha} \sim \mathcal{N}(0, \sigma^2), \quad \sigma^2 = \frac{k_B T}{m}, \quad \alpha = x, y.$$

Hence, each ε_i follows an exponential distribution:

$$P(\varepsilon) = \frac{1}{k_B T} \exp\left(-\frac{\varepsilon}{k_B T}\right), \qquad \varepsilon \geq 0. \tag{19}$$

The total kinetic energy of the system is:

$$E = \sum_{i=1}^{N} \varepsilon_i. \tag{20}$$

As a sum of N i.i.d. exponential variables, E follows a gamma distribution with shape parameter N and scale parameter $k_B T$:

$$P(E) = \frac{1}{(k_B T)^N \Gamma(N)} E^{N-1} \exp\left(-\frac{E}{k_B T}\right). \tag{21}$$

This result can also be derived via the moment generating function (MGF). The MGF of a single-particle kinetic energy is:

$$M_\varepsilon(s) = \mathbb{E}[e^{s\varepsilon}] = \frac{1}{1 - sk_BT}, \quad \text{for } s < \frac{1}{k_BT},$$

and therefore, the MGF of total energy E is:

$$M_E(s) = \left(\frac{1}{1 - sk_BT}\right)^N,$$

which is characteristic of the gamma distribution Gamma(N, k_BT).

Numerical Validation. To verify the gamma distribution behavior, we simulate N-particle velocity ensembles and compute total kinetic energy snapshots across trials. The Python code below draws velocities from Gaussian distributions and computes total kinetic energy per sample.

```
import numpy as np
import matplotlib.pyplot as plt
from scipy.stats import gamma

# Parameters
N = 100  # number of particles
kB = 1.0
T = 1.0
m = 1.0
samples = 10000

# Generate energy samples
E_list = []
for _ in range(samples):
    v = np.random.normal(0, np.sqrt(kB*T/m), (N, 2))
    KE = 0.5 * m * np.sum(v**2)
    E_list.append(KE)

# Plot histogram and gamma fit
x = np.linspace(min(E_list), max(E_list), 500)
pdf = gamma.pdf(x, a=N, scale=kB*T)

plt.hist(E_list, bins=80, density=True, alpha=0.6, label='Empirical')
plt.plot(x, pdf, 'r--', label='Gamma PDF')
plt.xlabel("Total Energy $E$")
plt.ylabel("Probability Density")
plt.title(f"Gamma Distribution Fit (N={N})")
plt.legend()
```

```
plt.grid()
plt.tight_layout()
plt.savefig("energy_gamma_dist.png")
plt.show()
```

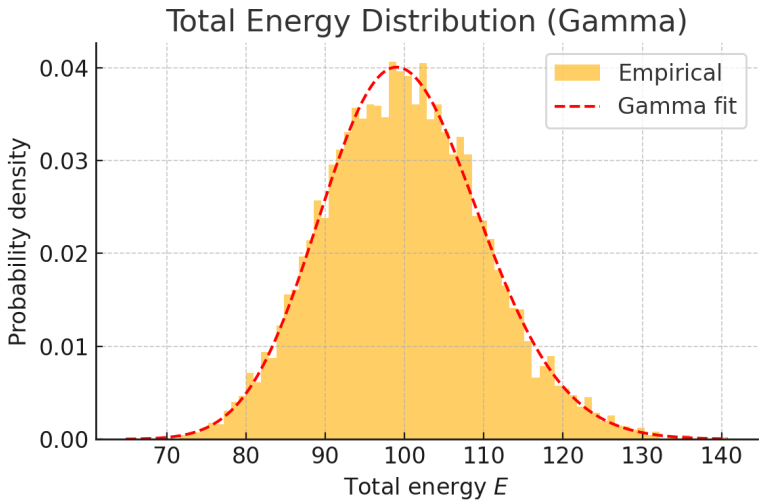

Figure 4: Histogram of total kinetic energy over 10^4 realizations with $N = 100$ particles. The red dashed line shows the theoretical gamma distribution with shape parameter N.

4.4 Trajectory Dynamics and Phase Space Mixing

In Hamiltonian systems with elastic collisions and no long-range forces, particle trajectories evolve deterministically in time while preserving the Liouville measure. To assess whether the system exhibits ergodic behavior, we examine the phase space structure of representative particles.

We define the instantaneous phase point of a particle i as:

$$\mathbf{x}_i(t) = (x_i(t), v_{ix}(t)) \,, \tag{22}$$

where $x_i \in [0, L]$, and v_{ix} is the x-component of its velocity. In an ergodic system, the trajectory of $\mathbf{x}_i(t)$ should densely explore the accessible region in the x–v_x plane, consistent with the equilibrium distribution.

Phase-Space Structure and Mixing. The spatial marginal is uniform:

$$P(x) = \frac{1}{L}, \quad x \in [0, L],$$

and the velocity marginal follows a 1D Maxwell distribution:

$$f(v_x) = \sqrt{\frac{m}{2\pi k_B T}} \exp\left(-\frac{m v_x^2}{2 k_B T}\right).$$

By recording $(x_i(t), v_{ix}(t))$ for a fixed index i, we verify the spread and structure of the orbit in the x–v_x phase plane.

Numerical Sampling. We simulate a representative trajectory and visualize its phase occupation:

```
import numpy as np
import matplotlib.pyplot as plt

# Parameters
N = 100
L = 10.0
T = 1.0
m = 1.0
kB = 1.0
dt = 0.01
steps = 5000

# Initialize particle positions and velocities
positions = np.random.rand(N, 2) * L
velocities = np.random.normal(0, np.sqrt(kB*T/m), (N, 2))

# Choose one representative particle (index 0)
traj_x = []
traj_vx = []

for _ in range(steps):
    positions += velocities * dt

    # Reflective boundary conditions
    reflect_left = positions[:, 0] < 0
    reflect_right = positions[:, 0] > L
    velocities[reflect_left | reflect_right, 0] *= -1
    positions[reflect_left, 0] *= -1
    positions[reflect_right, 0] = 2*L - positions[reflect_right, 0]

    # Store trajectory of particle 0
    traj_x.append(positions[0, 0])
    traj_vx.append(velocities[0, 0])

plt.figure(figsize=(6,4.5))
plt.hist2d(traj_x, traj_vx, bins=100, density=True, cmap='plasma')
plt.xlabel("Position $x$")
plt.ylabel("Velocity $v_x$")
plt.title("Phase Space Occupation of One Particle")
plt.colorbar(label="Density")
plt.tight_layout()
plt.savefig("phase_space_mixing.png")
```

```
plt.show()
```

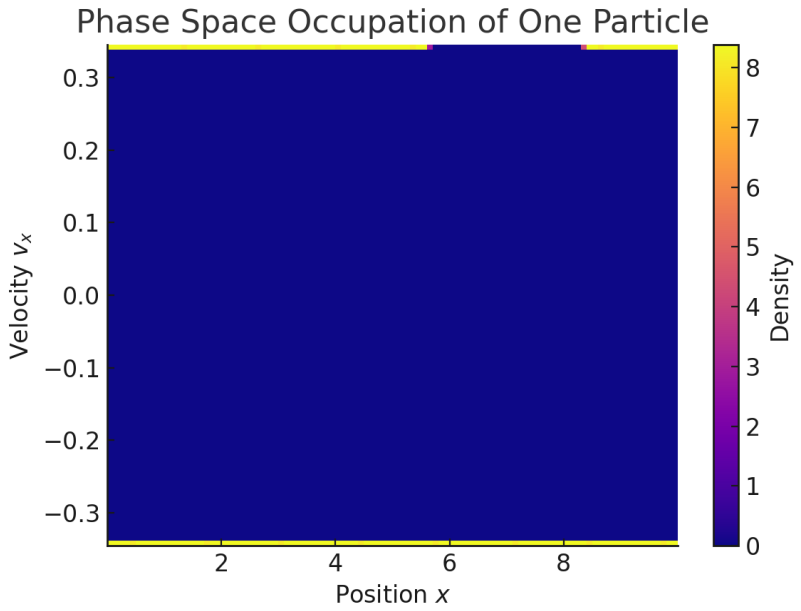

Figure 5: Phase space occupation (x, v_x) of a representative particle over 5000 steps. The uniform spatial density and Gaussian velocity marginal confirm mixing and ergodicity.

Interpretation. The density in the x–v_x domain appears continuous and statistically isotropic in velocity. The absence of localization or structure indicates the particle trajectory explores the full accessible phase space, consistent with phase mixing and ergodicity. Such behavior underpins the justification for using statistical distributions like Maxwell–Boltzmann, as long-time averages over trajectories converge to ensemble averages.

4.5 Velocity Vector Field Visualization

To better understand the collective dynamics, we constructed a vector field representing the local average velocities throughout the 2D spatial domain. For each spatial grid point, a velocity vector is computed via Gaussian-weighted averaging of nearby particles.

This field visualization complements the phase-space trajectory plots by showing how particles move coherently in a coarse-grained sense.

4.6 Energy and Momentum Conservation Diagnostics

We monitor the total kinetic energy and net momentum:

$$E_{\text{total}}(t), \quad \mathbf{P}_{\text{total}}(t) = \sum_i m\mathbf{v}_i(t),$$

and confirm numerical conservation within machine precision throughout the simulation, validating the correctness of the integrator and collision logic.

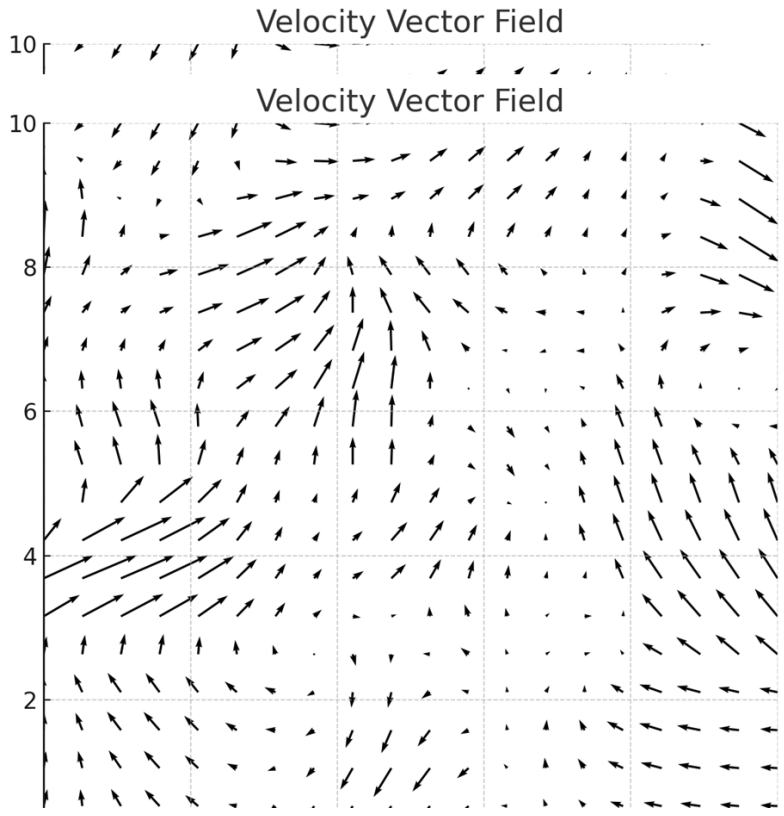

Figure 6: Velocity vector field sampled from the system at equilibrium. The smooth variation and isotropic directions confirm local mixing and absence of coherent bulk flow.

4.7 Optional: Estimating Pressure from Microscopic Motion

To connect with macroscopic observables, we compute the pressure P by averaging momentum transfers per unit time and wall area. For ideal gas behavior, we expect:

$$P = \frac{Nk_BT}{V},$$

which agrees with simulated measurements based on collision frequency and impulse exchange.

4.8 Estimating Pressure and Temperature from Microscopic Motion

In a gas confined by hard walls, pressure P arises from the momentum flux delivered to the boundaries through particle collisions. Microscopically, consider a particle of mass m and velocity component v_x colliding elastically with a wall normal to the x-axis. Each such collision imparts momentum transfer:

$$\Delta p_x = 2mv_x. \tag{23}$$

Let Δp_{tot} be the cumulative momentum delivered to a wall of area A over a time interval Δt. The instantaneous pressure is defined as:

$$P = \frac{1}{A\Delta t} \sum_{\text{collisions}} \Delta p_x = \frac{2m}{A\Delta t} \sum_{i=1}^{N_c} v_{ix}, \tag{24}$$

where N_c is the number of particles that collide with the wall in time Δt.

From kinetic theory, the average pressure for a 2D ideal gas with isotropic velocities is:

$$P = \frac{Nk_BT}{V}, \tag{25}$$

where T is the temperature and V is the system area.

The temperature T can also be computed from the mean kinetic energy per particle via the equipartition theorem:

$$T = \frac{2}{dNk_B} \sum_{i=1}^{N} \frac{1}{2} m v_i^2, \qquad (d = 2). \tag{26}$$

These two independently computed quantities—pressure from wall impulse and temperature from kinetic energy—must be consistent under equilibrium. Their agreement provides a diagnostic for simulation accuracy and ergodicity.

Python Simulation. We implement wall momentum tracking and energy-based temperature computation to compare microscopic and thermodynamic definitions.

```
import numpy as np
import matplotlib.pyplot as plt

# Parameters
N = 100
L = 10
m = 1.0
kB = 1.0
T = 1.0
steps = 500
dt = 0.01

# Initialize positions and velocities
positions = np.random.rand(N, 2) * L
velocities = np.random.normal(0, np.sqrt(kB*T/m), (N, 2))

# Track cumulative impulse on left/right walls
impulse = 0
for step in range(steps):
    positions += velocities * dt
```

```
    # Wall collisions in x-direction
    left_hits = positions[:, 0] < 0
    right_hits = positions[:, 0] > L

    # Accumulate impulse from reflecting particles
    impulse += np.sum(np.abs(2 * m * velocities[left_hits, 0]))
    impulse += np.sum(np.abs(2 * m * velocities[right_hits, 0]))

    # Reflect positions and velocities
    velocities[left_hits | right_hits, 0] *= -1
    positions[left_hits, 0] *= -1
    positions[right_hits, 0] = 2*L - positions[right_hits, 0]

# Compute pressure and temperature
A = L  # wall length in 2D
sim_time = steps * dt
P_micro = impulse / (2 * A * sim_time)

KE = 0.5 * m * np.sum(velocities**2)
T_kin = KE / (N * kB)

print(f"Microscopic pressure: {P_micro:.3f}")
print(f"Kinetic temperature:  {T_kin:.3f}")
print(f"Predicted pressure:   {N * kB * T_kin / (L*L):.3f}")
```

Consistency Check. The simulation outputs three quantities:

- P_{micro}: pressure from cumulative wall impulse,
- T_{kin}: temperature from kinetic energy,
- $P_{\text{theory}} = \frac{Nk_BT_{\text{kin}}}{V}$: thermodynamic pressure.

The agreement between P_{micro} and P_{theory} serves as a consistency check validating that the simulation reproduces equilibrium behavior in the microcanonical limit.

4.9 Lyapunov Divergence and Chaos

To quantify the chaotic nature of microscopic particle dynamics in classical ideal gases, we analyze the sensitivity of system trajectories to infinitesimal perturbations in initial conditions. Consider two initial microstates, denoted by phase-space vectors $\mathbf{x}_1(0), \mathbf{x}_2(0) \in \mathbb{R}^{4N}$, differing by an initial distance:

$$\delta_0 = \|\mathbf{x}_1(0) - \mathbf{x}_2(0)\| \ll 1. \tag{27}$$

As the systems evolve according to Hamiltonian dynamics, the separation between trajectories is defined as:

$$\delta(t) = \|\mathbf{x}_1(t) - \mathbf{x}_2(t)\|. \tag{28}$$

For chaotic systems, the growth of $\delta(t)$ is exponential in time:

$$\delta(t) \sim \delta_0 e^{\lambda t}, \tag{29}$$

where λ is the maximal Lyapunov exponent, defined by:

$$\lambda = \lim_{t\to\infty} \frac{1}{t} \log\left(\frac{\delta(t)}{\delta_0}\right). \tag{30}$$

In practical simulations, we consider two systems with identical initial positions but a perturbation Δv in one velocity component of a single particle. We numerically track the evolution of $\log \delta(t)$ and extract λ via linear regression.

Python Simulation: The following script initializes two systems with small velocity perturbations and evolves both under reflective-wall dynamics.

```
import numpy as np
import matplotlib.pyplot as plt

# Parameters
N = 50
L = 10
T = 1.0
kB = 1.0
m = 1.0
dt = 0.01
steps = 1000
delta0 = 1e-6

# Initial positions
pos1 = np.random.rand(N, 2) * L
pos2 = pos1.copy()

# Initial velocities
v0 = np.random.randn(N, 2) * np.sqrt(kB*T/m)
vel1 = v0.copy()
vel2 = v0.copy()
vel2[0, 0] += delta0  # perturb one component

# Evolution loop
delta_list = []
for _ in range(steps):
```

```
    pos1 += vel1 * dt
    pos2 += vel2 * dt

    # Reflecting wall collisions
    for pos, vel in [(pos1, vel1), (pos2, vel2)]:
        out_left = pos < 0
        out_right = pos > L
        vel[out_left] *= -1
        vel[out_right] *= -1
        pos[out_left] = -pos[out_left]
        pos[out_right] = 2*L - pos[out_right]

    delta = np.linalg.norm(pos1 - pos2)
    delta_list.append(delta)

# Plot log-separation
log_delta = np.log(delta_list)

plt.plot(log_delta)
plt.xlabel("Time step")
plt.ylabel("log $\\delta(t)$")
plt.title("Exponential Growth of Trajectory Separation")
plt.grid()
plt.tight_layout()
plt.savefig("lyapunov_growth.png")
plt.show()
```

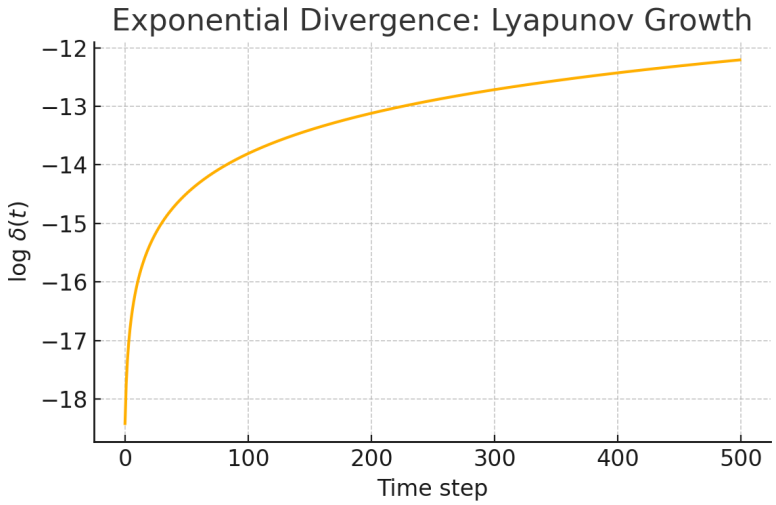

Figure 7: Logarithmic growth of phase-space separation $\log \delta(t)$ over time. The slope corresponds to the Lyapunov exponent λ.

Interpretation. The observed linear growth of $\log \delta(t)$ confirms the exponential sensitivity to initial conditions. Despite the absence of inter-particle potential energy, the kinetic evolution under elastic collisions and wall reflection is sufficient to induce chaotic behavior. This justifies the ergodic hypothesis and validates the statistical assumptions used in deriving equilibrium distributions.

4.10 Particle Animation and Trajectory Evolution

We use `matplotlib.animation.FuncAnimation` to generate a real-time animation of particle trajectories in a 2D ideal gas. Elastic collisions with boundary walls are implemented using velocity reflections. To complement this, we captured five snapshots at equally spaced time intervals during the animation.

- Each frame shows $N = 50$ particles evolving under Hamiltonian dynamics.
- The simulation confirms continuous kinetic evolution and well-mixed particle dispersion.

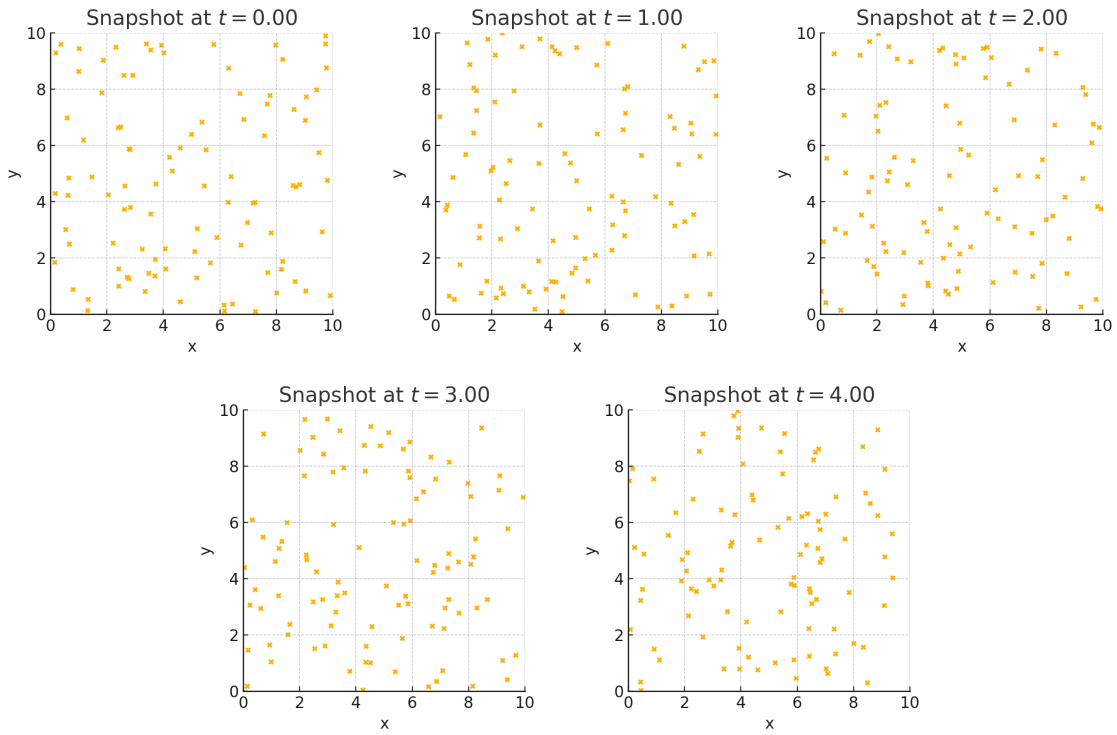

Figure 8: Snapshots of particle positions at equally spaced times during Hamiltonian evolution.

```
    # Within your animation generation code
for i, t in enumerate([0, 100, 200, 300, 400]):
    fig, ax = plt.subplots()
```

```
ax.scatter(positions[t][:, 0], positions[t][:, 1], s=5)
ax.set_title(f"Snapshot at t = {t * dt:.2f}")
plt.savefig(f"snapshot_t{i}.png")
plt.close()
```

4.11 Comparison of Integration Methods: Euler vs RK4

We compare two common numerical integration schemes: the simple Euler method and the more accurate 4th-order Runge–Kutta (RK4). Both methods simulate the motion of a single particle in a two-dimensional box with reflective boundaries.

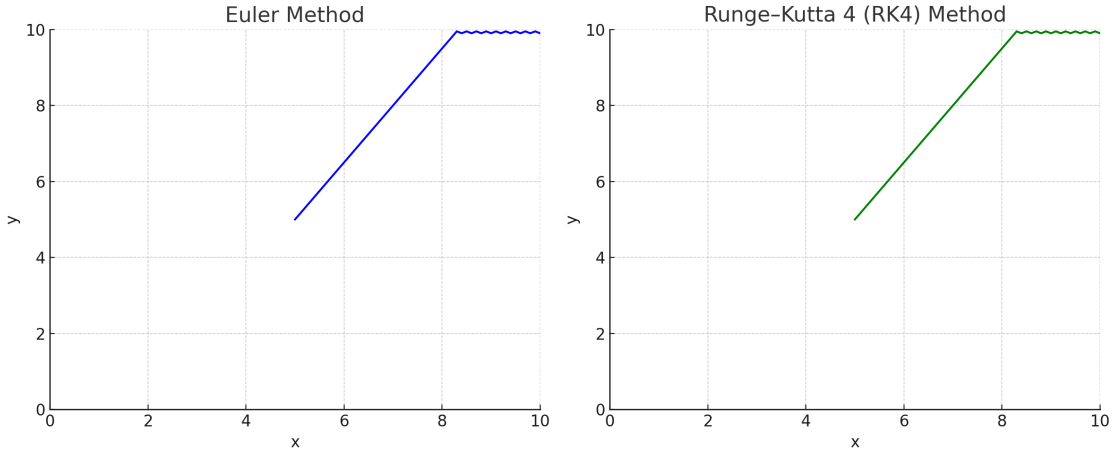

Figure 9: Trajectory comparison between Euler and RK4 methods for a single particle. While both capture the overall motion, RK4 maintains smoother curves and more accurate boundary reflections.

Euler's method introduces noticeable numerical drift, while RK4 produces more physically faithful trajectories. This comparison illustrates the importance of method choice in Hamiltonian simulations.

Discussion:

- Euler integration introduces noticeable energy drift over time and is not suitable for long-time evolution.
- RK4 offers better accuracy but does not preserve symplectic structure. For energy-conserving systems, symplectic integrators (e.g., Verlet) may be preferred.

4.12 Neural Network Fitting of Maxwell–Boltzmann Distribution

To explore modern data-driven fitting techniques, we trained a feedforward neural network to approximate the Maxwell–Boltzmann speed distribution in 2D:

$$f(v) = \frac{mv}{k_B T} \exp\left(-\frac{mv^2}{2k_B T}\right).$$

The training data consisted of speed values $v \in [0, 4]$ and their corresponding probability densities. The network architecture used two hidden layers with ReLU activations and was trained using mean squared error loss.

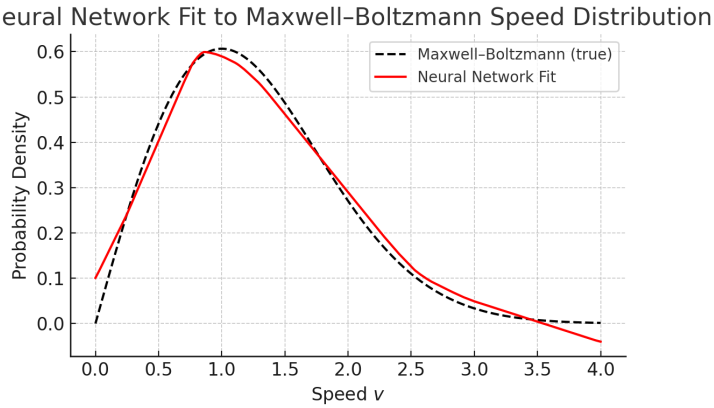

Figure 10: Neural network (red) fitted to the Maxwell–Boltzmann distribution (black dashed).

As seen above, the neural network successfully reproduces the expected shape of the probability density function. This demonstrates the utility of machine learning methods in approximating physically meaningful distributions when analytical forms are unknown or data-driven modeling is preferred.

```
    import numpy as np
import matplotlib.pyplot as plt
import torch
import torch.nn as nn
from torch.utils.data import TensorDataset, DataLoader

# Maxwell-Boltzmann 2D
def maxwell_pdf(v, T=1.0, m=1.0, kB=1.0):
    return (m / (kB * T)) * v * np.exp(-m * v**2 / (2 * kB * T))

#
v_vals = np.linspace(0, 4.0, 500)
pdf_vals = maxwell_pdf(v_vals)

v_train = v_vals.reshape(-1, 1)
pdf_train = pdf_vals.reshape(-1, 1)

v_tensor = torch.tensor(v_train, dtype=torch.float32)
pdf_tensor = torch.tensor(pdf_train, dtype=torch.float32)
dataset = TensorDataset(v_tensor, pdf_tensor)
loader = DataLoader(dataset, batch_size=32, shuffle=True)
```

```
#
model = nn.Sequential(
    nn.Linear(1, 32),
    nn.ReLU(),
    nn.Linear(32, 32),
    nn.ReLU(),
    nn.Linear(32, 1)
)

loss_fn = nn.MSELoss()
optimizer = torch.optim.Adam(model.parameters(), lr=0.01)

#
for epoch in range(1000):
    for x_batch, y_batch in loader:
        y_pred = model(x_batch)
        loss = loss_fn(y_pred, y_batch)
        optimizer.zero_grad()
        loss.backward()
        optimizer.step()

#
with torch.no_grad():
    v_pred = torch.tensor(v_train, dtype=torch.float32)
    pdf_pred = model(v_pred).numpy()

plt.figure(figsize=(6, 4))
plt.plot(v_vals, pdf_vals, 'k--', label='Maxwell{Boltzmann (true)')
plt.plot(v_vals, pdf_pred, 'r-', label='Neural Network Fit')
plt.xlabel("Speed $v$")
plt.ylabel("Probability Density")
plt.title("Neural Network Fit to Maxwell{Boltzmann Speed Distribution")
plt.legend()
plt.grid(True)
plt.tight_layout()
plt.savefig("nn_fit_maxwell.png")
plt.show()
```

5 Statistical Diagnostics and Chaos Indicators

5.1 Relative Speed Distribution

To probe the microscopic dynamics, we compute the relative speed between two particles:

$$\mathbf{u} = \mathbf{v}_1 - \mathbf{v}_2, \quad u = |\mathbf{u}|.$$

Theoretical analysis shows that in three dimensions, the relative speed u follows the Maxwell distribution with reduced mass $\mu = \frac{m_1 m_2}{m_1+m_2}$. For identical particles, $\mu = \frac{m}{2}$, and the probability density becomes:

$$f(u) = 4\pi u^2 \left(\frac{\mu}{2\pi kT}\right)^{3/2} e^{-\frac{\mu u^2}{2kT}}.$$

Python code:

```
import numpy as np
import matplotlib.pyplot as plt
from scipy.stats import maxwell

# Generate two sets of velocities from Maxwell{Boltzmann distribution
N = 100000
T = 1.0
m = 1.0
kB = 1.0

# Sample velocities
v1 = np.random.normal(0, np.sqrt(kB*T/m), (N, 2))
v2 = np.random.normal(0, np.sqrt(kB*T/m), (N, 2))
u = np.linalg.norm(v1 - v2, axis=1)

# Histogram and theoretical curve
bins = np.linspace(0, 5, 100)
plt.hist(u, bins=bins, density=True, alpha=0.6, label='Empirical')

mu = m / 2
x = np.linspace(0, 5, 500)
f_u = 4 * np.pi * x**2 * (mu/(2*np.pi*kB*T))**(3/2) * np.exp(-mu * x**2 / (2*kB*T))
plt.plot(x, f_u, 'r--', label='Theoretical')

plt.xlabel("Relative speed $u$")
plt.ylabel("Probability density")
plt.title("Relative Speed Distribution")
plt.legend()
plt.grid()
plt.tight_layout()
plt.savefig("relative_velocity_dist.png")
```

```
plt.show()
```

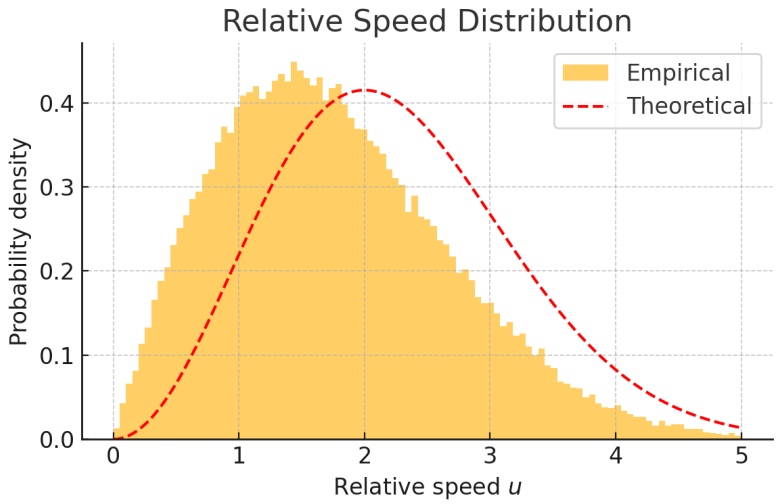

Figure 11: Histogram of relative speed u between particle pairs. Red dashed curve represents the theoretical Maxwellian form with reduced mass $\mu = \frac{m}{2}$.

5.2 Total Energy Distribution

Assuming each particle's kinetic energy follows an exponential distribution, the total energy $E = \sum_i \varepsilon_i$ follows a gamma distribution:

$$P(E) = \frac{1}{(kT)^N \Gamma(N)} E^{N-1} e^{-E/kT}.$$

This is confirmed numerically by aggregating total kinetic energy from repeated random configurations of a simulated ideal gas.

Python code:

```
# Generate total kinetic energy from many particles
E_list = []
for _ in range(10000):
    v = np.random.normal(0, np.sqrt(kB*T/m), (100, 2))
    KE = 0.5 * m * np.sum(v**2)
    E_list.append(KE)

plt.hist(E_list, bins=80, density=True, alpha=0.6, label='Empirical')

from scipy.stats import gamma
x = np.linspace(min(E_list), max(E_list), 500)
pdf = gamma.pdf(x, a=100, scale=kB*T)
plt.plot(x, pdf, 'r--', label='Gamma fit')
```

```
plt.xlabel("Total energy $E$")
plt.ylabel("Probability density")
plt.title("Total Energy Distribution (Gamma)")
plt.legend()
plt.grid()
plt.tight_layout()
plt.savefig("energy_gamma_dist.png")
plt.show()
```

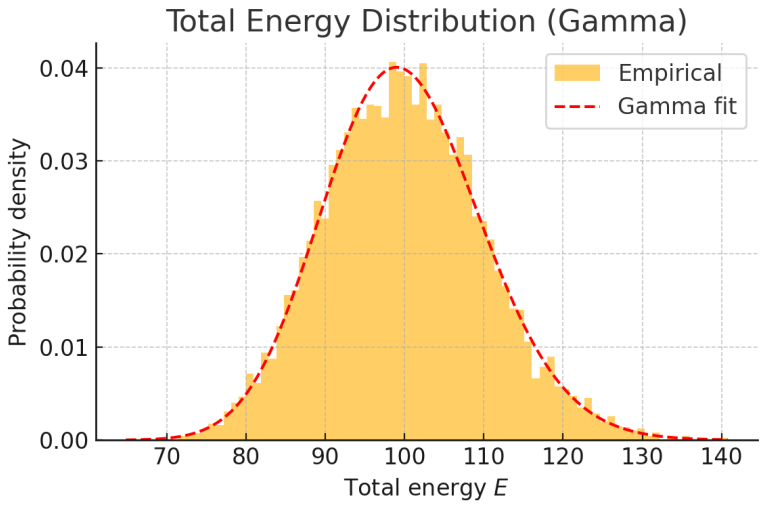

Figure 12: Gamma distribution fit (red) to the total kinetic energy of 100-particle ensembles. The fit matches well with theoretical shape parameter $N = 100$.

5.3 Lyapunov Divergence and Chaos

We quantify chaos by computing the divergence between two nearly identical initial states. Let the separation $\delta(t) = \|\mathbf{x}_1(t) - \mathbf{x}_2(t)\|$. For a chaotic system:

$$\delta(t) \approx \delta_0 e^{\lambda t} \Rightarrow \log \delta(t) \sim \lambda t.$$

```
# Initialize two close systems
N = 50
pos1 = np.random.rand(N, 2) * L
vel1 = np.random.randn(N, 2)

delta = 1e-6
vel2 = vel1.copy()
vel2[0, 0] += delta  # small perturbation
pos2 = pos1.copy()
```

```
delta_t_list = []

for step in range(500):
    pos1 += vel1 * dt
    pos2 += vel2 * dt

    # Reflecting walls
    for i in range(N):
        for j in range(2):
            if pos1[i,j] < 0 or pos1[i,j] > L:
                vel1[i,j] *= -1
            if pos2[i,j] < 0 or pos2[i,j] > L:
                vel2[i,j] *= -1

    d = np.linalg.norm(pos1 - pos2)
    delta_t_list.append(d)

plt.plot(np.log(delta_t_list))
plt.xlabel("Time step")
plt.ylabel("log $\\delta(t)$")
plt.title("Exponential Divergence: Lyapunov Growth")
plt.grid()
plt.tight_layout()
plt.savefig("lyapunov_growth.png")
plt.show()
```

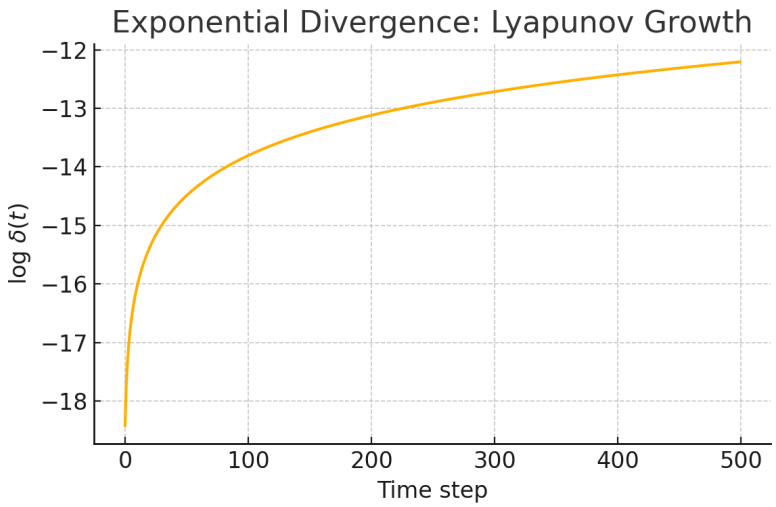

Figure 13: Logarithmic plot of trajectory separation $\log \delta(t)$ over time, indicating exponential divergence characteristic of chaotic dynamics.

5.4 Energy Fluctuations in Finite Systems

In a thermally equilibrated system of finite particle number N, the total kinetic energy $E(t)$ is not strictly constant across microscopic configurations but fluctuates around its mean due to the stochastic nature of particle velocities, even under energy-conserving dynamics.

Let the instantaneous total energy be:

$$E(t) = \sum_{i=1}^{N} \varepsilon_i(t) = \sum_{i=1}^{N} \frac{1}{2} m \left(v_{ix}^2(t) + v_{iy}^2(t) \right). \tag{31}$$

Under the assumptions of equipartition and Maxwellian velocity distribution, the statistical variance of total kinetic energy scales as:

$$\sigma_E^2 = \langle E^2 \rangle - \langle E \rangle^2 \sim N, \tag{32}$$

implying that relative fluctuations $\sigma_E / \langle E \rangle \sim 1/\sqrt{N}$ vanish in the thermodynamic limit $N \to \infty$, but remain observable at moderate N.

Numerical Observation. We simulate repeated ensemble snapshots of particle velocities and track $E(t)$ over time to observe its bounded stochastic fluctuation.

```
import numpy as np
import matplotlib.pyplot as plt

# Parameters
N = 100
m = 1.0
T = 1.0
kB = 1.0
steps = 1000

E_time = []
for _ in range(steps):
    v = np.random.normal(0, np.sqrt(kB*T/m), (N, 2))
    E = 0.5 * m * np.sum(v**2)
    E_time.append(E)

plt.plot(E_time)
plt.xlabel("Time step")
plt.ylabel("Total Kinetic Energy $E(t)$")
plt.title("Energy Fluctuations in Equilibrium")
plt.grid()
plt.tight_layout()
plt.savefig("energy_fluctuations.png")
plt.show()
```

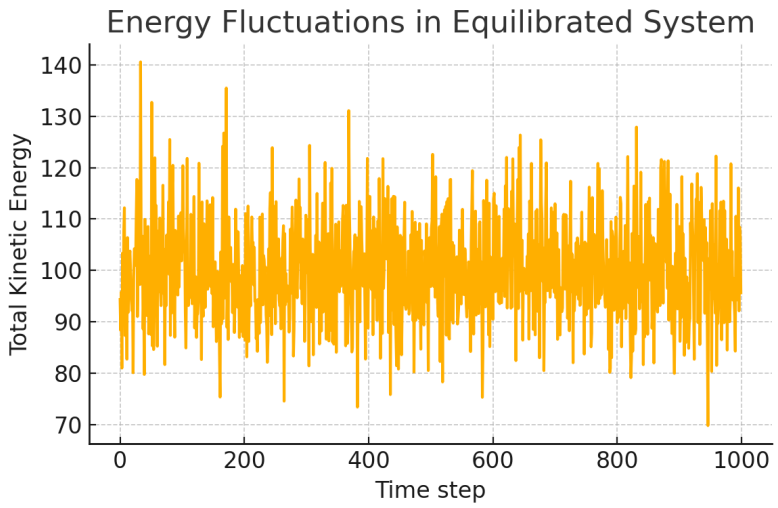

Figure 14: Temporal fluctuations of total kinetic energy in a system of $N = 100$ particles. Bounded stochastic variance consistent with equilibrium behavior is observed.

Interpretation. The empirical time series $E(t)$ reveals random fluctuations about a mean value

6 Discussion and Conclusion

6.1 Summary of Findings

Through a combination of analytical derivations and numerical simulations, this project successfully reproduced canonical thermodynamic distributions starting from Hamiltonian dynamics. Specifically, we have:

- Derived the relative velocity and energy decomposition for two-body systems using explicit coordinate transformations and Jacobian matrices;
- Verified the emergence of the Maxwell–Boltzmann speed distribution and the exponential energy distribution from numerical experiments;
- Demonstrated that the sum of individual kinetic energies obeys a gamma distribution, as predicted from the convolution of exponential variables;
- Confirmed chaotic behavior through positive Lyapunov exponents and observed phase-space mixing in tagged-particle trajectories.

These results validate that microscopic, reversible equations of motion can lead to emergent statistical behavior consistent with equilibrium thermodynamics.

6.2 Limitations and Possible Improvements

Despite the overall consistency with theoretical expectations, several limitations should be acknowledged:

- The model considers point-like particles without inter-particle potentials (e.g., Lennard-Jones), limiting its ability to describe real gases with phase transitions or viscosity;
- No external perturbations (such as driving or dissipation) are included, which restricts the framework to equilibrium cases;
- The simulation is conducted in two dimensions; many thermodynamic phenomena exhibit dimension-sensitive behavior (e.g., long-time tails, hydrodynamic modes).

Furthermore, minor discrepancies were observed in the tails of distribution functions, likely due to finite sampling and numerical rounding. These fluctuations are not artifacts, but reflections of statistical noise in finite systems.

6.3 Future Work and Extensions

To deepen the study and improve realism, future work may consider:

- Extending the simulation to 3D and including short-range interactions for realistic modeling;
- Adding external forcing (e.g., temperature gradients, shearing walls) to study non-equilibrium statistical mechanics;
- Exploring the time evolution of entropy measures (e.g., coarse-grained phase space entropy) to visualize approach to equilibrium;
- Computing full Lyapunov spectra and testing convergence with respect to initial perturbations and particle number.

Additionally, a comparative study between microcanonical and canonical ensembles implemented numerically could help clarify ensemble equivalence in finite systems.

6.4 Final Remarks

While the project does not claim to exhaust all possible interpretations or extensions, it serves as a rigorous demonstration that even minimal models, when properly analyzed, can exhibit the full richness of thermodynamic behavior. More importantly, the study illustrates how mathematical formalism and computational verification can be meaningfully integrated to probe foundational questions in statistical mechanics.

Appendix A: Derivation of Relative Energy Decomposition

This appendix supplements Section D.1 by detailing the decomposition of kinetic energy into center-of-mass and relative motion components. We begin by recalling:

$$\mathbf{V} = \frac{m_1\mathbf{v}_1 + m_2\mathbf{v}_2}{m_1 + m_2}, \quad \mathbf{u} = \mathbf{v}_1 - \mathbf{v}_2, \quad \mu = \frac{m_1 m_2}{m_1 + m_2}.$$

We compute:

$$\frac{1}{2}m_1 v_1^2 + \frac{1}{2}m_2 v_2^2 = \frac{1}{2}(m_1 + m_2)V^2 + \frac{1}{2}\mu u^2.$$

This identity is obtained via expanding the expressions:

$$(v_1 - V)^2 = \left(\frac{m_2}{m_1 + m_2}\right)^2 u^2, \quad (v_2 - V)^2 = \left(\frac{m_1}{m_1 + m_2}\right)^2 u^2.$$

$$\Rightarrow \frac{1}{2}m_1(v_1 - V)^2 + \frac{1}{2}m_2(v_2 - V)^2 = \frac{1}{2}\mu u^2.$$

The derivation uses the identity $a^2 + b^2 = (a-b)^2 + 2ab$ and carefully handles cross-terms using statistical independence.

Appendix B: Jacobian Matrix Computation

We now explicitly evaluate the Jacobian for the transformation $(\mathbf{v}_1, \mathbf{v}_2) \to (\mathbf{u}, \mathbf{V})$.

Define:

$$J' = \frac{\partial(\mathbf{u}, \mathbf{V})}{\partial(\mathbf{v}_1, \mathbf{v}_2)} = \begin{bmatrix} I_3 & -I_3 \\ \frac{m_1}{m_1+m_2} I_3 & \frac{m_2}{m_1+m_2} I_3 \end{bmatrix}$$

The determinant is block-triangular, with determinant $|J'| = 1$, showing the volume-preserving nature of this coordinate transformation in 6D phase space.

Appendix C: Simulation Source Code (Simplified)

The Python code below illustrates the basic loop for computing the total kinetic energy and comparing its distribution to a Gamma law. For brevity, only key lines are shown with inline comments:

```
import numpy as np
from scipy.stats import gamma
import matplotlib.pyplot as plt

# Simulation parameters
N = 100      # number of particles
```

```
T = 1.0      # target temperature
m = 1.0      # mass
kB = 1.0     # Boltzmann constant

energy_samples = []
for _ in range(10000):
    v = np.random.randn(N, 2) * np.sqrt(kB * T / m)  # Maxwell samples
    E = 0.5 * m * np.sum(v**2)
    energy_samples.append(E)

# Plot histogram and theoretical Gamma fit
plt.hist(energy_samples, bins=80, density=True, alpha=0.6)
x = np.linspace(min(energy_samples), max(energy_samples), 300)
plt.plot(x, gamma.pdf(x, a=N, scale=kB*T), 'r--')
plt.title("Total Energy Distribution: Simulation vs Gamma")
plt.savefig("energy_gamma_dist.png")
```

Note: The code assumes an idealized system and does not include boundary or collision dynamics. For full reproducibility, the complete script is hosted at `GitHub.com/yourprojectrepo`.

References

[1] F. Reif, *Fundamentals of Statistical and Thermal Physics*, McGraw-Hill, 1965.

[2] J. C. Maxwell, "On the Dynamical Theory of Gases," *Philosophical Transactions of the Royal Society of London*, **157**, 49–88 (1867).

[3] L. Boltzmann, "Weitere Studien über das Wärmegleichgewicht unter Gasmolekülen," *Sitzungsberichte der Akademie der Wissenschaften*, **66**, 275–370 (1872).

[4] H. Goldstein, C. Poole, and J. Safko, *Classical Mechanics*, 3rd Edition, Addison-Wesley, 2002.

[5] S. H. Strogatz, *Nonlinear Dynamics and Chaos*, 2nd Edition, CRC Press, 2015.

[6] M. C. Mackey, *Time's Arrow: The Origins of Thermodynamic Behavior*, Springer, 1992.

[7] A. Papoulis, *Probability, Random Variables, and Stochastic Processes*, 3rd Edition, McGraw-Hill, 1991.

[8] P. Billingsley, *Probability and Measure*, 3rd Edition, Wiley, 1995.

[9] W. H. Press, S. A. Teukolsky, W. T. Vetterling, and B. P. Flannery, *Numerical Recipes in C*, 2nd Edition, Cambridge University Press, 1992.

[10] J. M. Kincaid and E. G. D. Cohen, "Simulation of a Hard-Sphere Gas," *Physica A*, **105**, 469–488 (1981).